The inhibition of CO_2 corrosion of L360 mild steel in 3.5% NaCl solution by imidazoline derivatives

A.I. Obike,[1,2,3]* P.C. Okafor,[2] K.J. Uwakwe,[2] X. Jiang[3] and D. Qu[3]

[1]*Department of Pure & Industrial Chemistry, Abia State University, Uturu, Abia State, Nigeria*

[2]*Corrosion and Electrochemistry Research Group, Department of Pure & Applied Chemistry, University of Calabar, Calabar, Nigeria*

[3]*SINOPEC Research Institute of Safety Engineering, 218, Yan'an 3rd RD, Qingdao, P.R. China, 266071*

**E-mail: anthonyobike@yahoo.com*

Abstract

[2-(2-Henicos-10-enyl-4,5-dihydro-imidazol-1-yl)-ethyl]-methylamine (HDM), 2-(2-henicos-10-enyl-4,5-dihydro-imidazol-1-yl)-ethanol (HDE) and 2-henicos-10-enyl-4,5-dihydro-1*H*-imidazole (HDI) were synthesized using the solvent free microwave assisted organic synthesis method and characterized by FT-IR. The corrosion inhibition properties of these compounds on mild steel L360 in 3.5% NaCl solution were investigated by weight loss, potentiodynamic polarization, electrochemical impedance and scanning electron microscopic techniques. The synthesized inhibitors were tested at 60°C and 80°C with concentrations of 10, 50, 100, 200 and 300 ppm, respectively. The results from the study showed that the inhibition efficiency increased with increase in the concentration of the inhibitor to a maximum and decreased with rise in temperature. An adherent layer of inhibitor molecules on the surface is proposed to account for their inhibitive action in which the organic molecules adsorb on the active anodic and cathodic sites following Langmuir isotherm. The effectiveness of these inhibitors has been correlated to their chemical structures and were in the order of HDM > HDE > HDI. The values of activation energy, free energy of adsorption and heat of adsorption were also calculated to elaborate the mechanism of corrosion inhibition. The values obtained from the heat of adsorption (Q_{ads}) for the three inhibitors studied (HDM, HDE and HDI) are –58.53 kJ mol^{-1}, –103.27 kJ mol^{-1} and –133.67 kJ mol^{-1}, respectively. These negative values indicate that the adsorption of the inhibitors on the mild steel is exothermic signifying physical adsorption. The potentiodynamic polarization data show that the compounds studied are mixed type inhibitors. The surface characteristics of inhibited and uninhibited metal samples were investigated by scanning electron microscopy (SEM).

Received: February 16, 2018. Published: July 22, 2018 doi: 10.17675/2305-6894-2018-7-3-3

Keywords: *corrosion; corrosion inhibition; imidazoline derivative; mild steel; adsorption.*

1. Introduction

Carbon dioxide (CO_2) is a serious problem in the oil and gas industry as it is usually encountered in wells during oil and gas exploration. This problem leads to reduced production and expensive maintenance and repairs running into billions of dollars yearly [1, 2]. The use of inhibitors has proved to be an effective means of corrosion control. Organic compounds as inhibitors have been found to be not only economical but also environmentally friendly compared to its inorganic counterpart [3]. Organic compounds are usually obtained by either extraction from natural sources or by synthesis, and those containing oxygen, sulfur and nitrogen have been shown to be effective in reduction of corrosive attacks on mild steel [4–7]. Imidazoline ring framework contains nitrogen with a lone pair of electron with which it is adsorbed on the metal surface. The alkyl amine substituent of the imidazoline ring acts like an anchor and helps to maintain its adsorption on the metal surface; the 'tail' part is the long hydrocarbon chain which provides hydrophobic film on the metal surface thus providing inhibition [8–11]. In continuation of an ongoing research in our laboratory on synthesis and inhibitive action of imidazoline derivatives we present here, synthesis and inhibition behavior of [2-(2-henicos-10-enyl-4,5-dihydro-imidazol-1-yl)-ethyl]-methylamine (HDM), 2-(2-henicos-10-enyl-4,5-dihydro-imidazol-1-yl)-ethanol (HDE) and 2-henicos-10-enyl-4,5-dihydro-1*H*-imidazole (HDI). The primary focus of this work is the assessment of the inhibition behavior of these inhibitors on mild steel and an initial assessment of the mechanism by which it occurred.

2. Experimental details

2.1 Sample (mild steel)

L360 mild steel specimens were cut from unused petroleum pipeline as regular edged cuboids with dimension (2.0×0.4×0.1 inch). The alloy had the weight percentage chemical composition as shown in Table 1. Before the electrochemical and gravimetric measurements, the iron samples were polished using different grits of silicon carbide abrasive paper (240; 400, 600 and 800 grits) and cleaned with acetone, washed with double-distilled water and finally dried with hot air.

Table 1. Chemical composition of mild steel L360.

Element	V	Cr	Mn	Ni	Cu	Mo	W	Fe
Composition (wt %)	0.06	0.05	1.09	0.00	0.10	0.09	0.00	96.55

2.2 Inhibitors

The organic compounds tested as corrosion inhibitors were synthesized by the authors using the solvent free microwave assisted organic synthesis method. The method used is a modification of that previously used by Usyatinsky and Khmelnitsky [12]. Fatty acid (behenic acid) was reacted with different vicinal amine compounds: diethylenetriamine

(DETA), ethylenediamine (EDA) and aminoethylethanolamine (AEEA). The obtained products were purified, and characterized by FT-IR. Melting points were obtained using open capillary tubes. Reaction procedure is as shown in Equation 1. "X" in the reaction scheme is the alkyl amine substituent and "R" is the long hydrocarbon chain from the fatty acid.

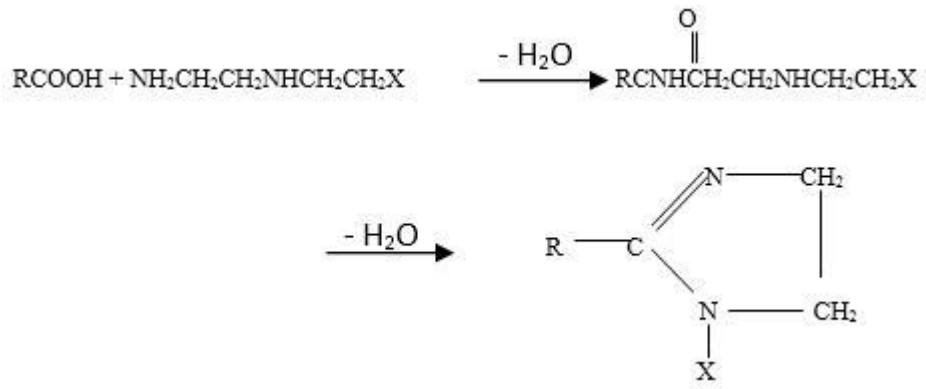

(1)

Figure 1. Imidazoline derivative synthesis reaction scheme.

Table 2. List of synthesized inhibitors.

Reaction	Name	Abbreviation	Structures	Molecular weight	Melting point
Behenic acid + DETA	[2-(2-Henicos-10-enyl-4,5-dihydro-imidazol-1-yl)-ethyl]-methylamine	HDM	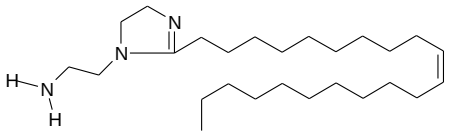	406.70	73–77
Behenic acid + AEEA	2-(2-Henicos-10-enyl-4,5-dihydro-imidazol-1-yl)-ethanol	HDE	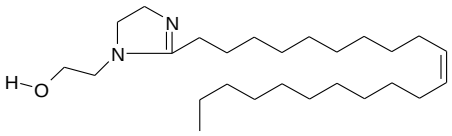	419.74	71–78
Behenic acid + EDA	2-Henicos-10-enyl-4,5-dihydro-1H-imidazole	HDI	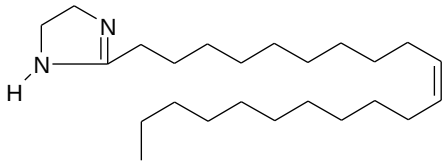	362.65	71–76

2.3 Attack solution

The aggressive solution, 3.5% NaCl, was prepared by dissolving of analytical grade NaCl in distilled water.

2.4 Gravimetric method

For weight loss measurements, the specimens were pre-weighed and suspended in 250 ml of the test solutions (3.5% NaCl solution in the absence and presence of inhibitor) with the help of glass hooks and rods at 80±1°C (at this temperature all the inhibitors would have dissolved very well in the test medium). The specimens were retrieved at 24 h intervals, carefully washed in 20% NaOH solution containing 200 g L^{-1} of zinc dust, rinsed in distilled water, air dried after dipping in acetone and re-weighed [7, 9]. The procedure was repeated for upwards of 3 days. The weight loss was determined as the difference in weight of the mild steel specimens before and after immersion in different test solutions. The inhibition efficiency *E* % was calculated by the relation:

$$E\,\% = \left(i_{\text{corr}} - \frac{i_{\text{corr(inh)}}}{i_{\text{corr}}} \right) \times 100 = \left(R_{\text{ct(inh)}} - \frac{R_{\text{ct}}}{R_{\text{ct(inh)}}} \right) \times 100 = \left(R_{\text{p(inh)}} - \frac{R_{\text{p}}}{R_{\text{p(inh)}}} \right) \times 100 \qquad (2)$$

where, i_{corr} is corrosion current, R_{ct} is charge transfer resistance, R_{p} is polarization resistance and (inh) means inhibited / with inhibitor.

2.5 LPR, EIS and PDP measurements

Experiments were conducted using a conventional three-electrode 2000 ml glass cell setup, with the counter electrode made of a platinum foil and a saturated Ag/AgCl reference electrode used as the reference electrode. This was connected externally to the cell *via* a Luggin capillary tube and a porous tip. The glass cell was filled with 1800 ml of the test solution, deaerated, and saturated with carbon dioxide at atmospheric pressure of 1 bar for two hours. The pH was adjusted to 5.5 in each case with hydrochloric acid (HCl) or sodium hydroxide (NaOH), as the case may be. The pH was monitored before and after addition of inhibitor to ensure constant solution composition. The working electrode was immersed for 1 hour prior to each experimental measurement to attain a stable potential within ±1 mV. LPR was conducted by polarizing the working electrode ±5 mV *versus* the open-circuit potential at a rate of 0.125 mV/s followed by EIS measurements over the frequency range 100 kHz to 10 mHz with a signal amplitude perturbation of 5 mV/s. The potentiodynamic polarization sweeps were conducted at a sweep rate of 0.5 mV/s. The solution and metal coupons were changed after each sweep. Measurements were taken at this time to avoid the interaction of corrosion product with inhibitor films with increased time. Experiments were carried out in duplicates and triplicates for each experimental condition. Synthesized inhibitors were tested at 60°C and 80°C (these temperatures were used to facilitate the dissolution of the inhibitors in the test solution) with concentrations of 10, 50, 100, 200 and 300 ppm.

3. Results and Discussion

3.1 Structure elucidation and corrosion inhibition behavior of HDM, HDE and HDI

Table 3 shows the FT-IR bands in cm^{-1} for HDM, HDE and HDI. The structure of imidazoline compound was identified by FT-IR within the wave number 400–4000 cm^{-1}. A sample of spectrum obtained is shown in Figure 2.

Table 3. FT-IR bands (cm^{-1}) for HDM, HDE and HDI.

Compounds	NH_2	NH	OH	–C–H CH_2, CH_3	C=N	Imidazoline ring	N=C–N	$(CH_2)_n$ skeletal
HDM	3303			2924	1648	1609	1550	720
HDE			3100	2952	1664	1607	1553	720
HDI		3291		2924	1656	1608	1554	723

As illustrated by the Figure, there are obvious absorbing peaks around 720, 1550, 1607, 1650, 2924, and 3291 cm^{-1} respectively. These peaks correspond to $(CH_2)_n$ skeletal frame work, double bond N=C–N stretching vibration, imidazoline ring, C=N stretching vibration, alkyl and ethylene group and NH stretching vibration respectively. In other FT-IR spectrums obtained for HDM and HDE absorption peaks were observed at 3303 and 3100 corresponding to NH_2 and OH stretching vibrations respectively. Therefore, imidazoline compound belongs to pentaimidazolinium compounds. These observations were generally in agreement with the expected correlations [11, 13, 14].

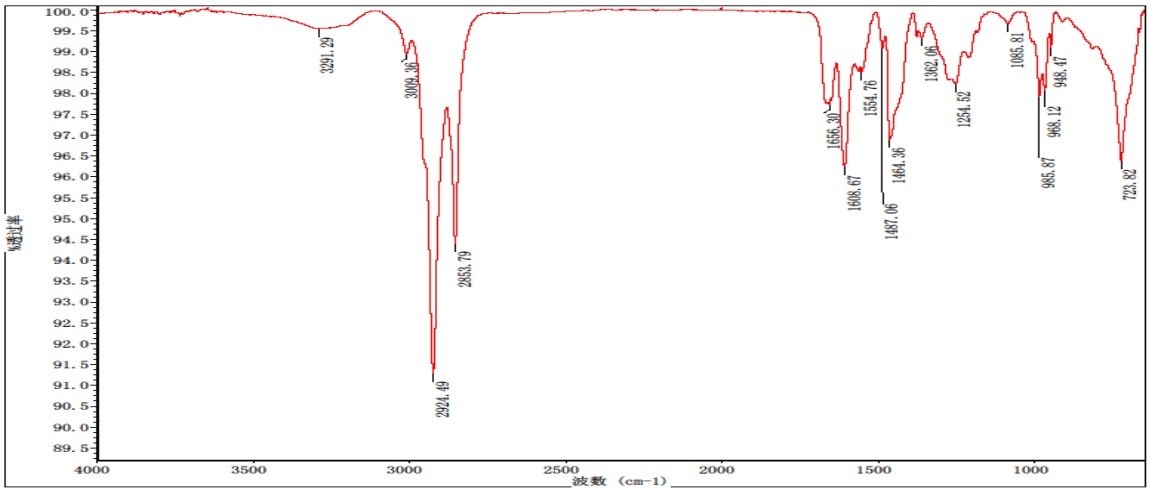

Figure 2. FT-IR spectrum obtained for HDI.

The polarization curves obtained for L360 mild steel in CO_2 saturated 3.5% NaCl solution in the absence and presence of different concentrations of HDM at 60°C and 80°C

are shown in Figure 3. It is observed from the curves that the profile of the curves in the absence and presence of the inhibitors are different, in the presence of inhibitors more linear cathodic curves are observed and the anodic curves are observed to be irregular with two linear portions suggesting that the inhibitors adsorbed onto the metal surface and retards corrosion by blocking the active sites and altering the anodic and cathodic reaction mechanisms [15]. From this curves and other curves obtained for HDE and HDI, corrosion potential (E_{corr}) and corrosion current density (i_{corr}) were deduced these results are shown in Table 4. The i_{corr} was used to calculate the inhibition efficiency using the formula shown in Equation 2.

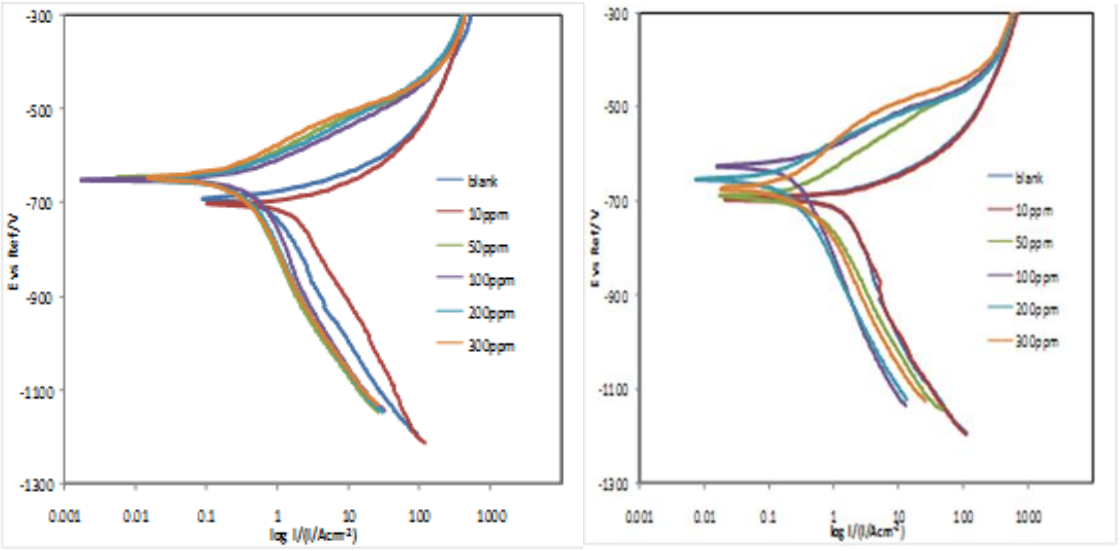

(a) (b)

Figure 3. Polarization curves obtained at (a) 60°C and (b) 80°C for L360 mild steel in CO_2 saturated 3.5% NaCl solutions in the absence and presence of HDM at 60°C.

The inhibition efficiency results obtained are shown in Table 5. The results indicate that the presence of the compounds inhibited the corrosion processes without evidence of passivation on the anode, in both blank and inhibited solutions within the studied potentials. It is observed from Figure 3 that both the anodic and cathodic reactions are affected, based on this, the compounds are considered as mixed type inhibitors.

The Nyquist plots for L360 for L360 mild steel in CO_2 saturated 3.5% NaCl solution in the absence and presence of different concentrations of HDM at 60°C and 80°C are shown in Figure 4. In the absence of inhibitors, the Nyquist plots obtained do not differ significantly from each other and are both characterized by a high frequency capacitive and low frequency inductive loops at the two temperatures studied. The high frequency (with centre under the real axis) is the characteristic of solid electrodes and has been attributed to roughness and other inhomogeneities of the electrode [15]. The high frequency capacitive loop may also be attributed to the double layer capacity in parallel with charge transfer resistance. Though it is probably a composite value representing dissolution of the iron and

other alloying elements, it is governed by the dissolution of iron since iron is the major component of the alloys [15, 16]. The inductive loop is ascribed to the adsorption of species exhibiting negative change in the surface coverage with potential on the surface of the metal [14, 15].

Table 4. Polarization parameters.

Inhibitor	Conc. (ppm)	Polarization Parameters					
		E_{corr} (mV)		i_{corr} (μA cm^{-2})		Θ	
		60°C	80°C	60°C	80°C	60°C	80°C
BLANK	0	–693.0	–694.1	81.97	121.4		
HDM	10	–680.2	–705.1	53.78	82.08	0.30	0.32
	50	–646.3	–704.9	30.49	81.61	0.63	0.33
	100	–649.6	–692.6	54.98	38.77	0.33	0.68
	200	–644.8	–698.6	32.30	30.14	0.60	0.75
	300	–651.6	–689.8	37.48	46.95	0.54	0.61
HDE	10	–692.8	–688.5	83.14	70.48	–0.01	0.41
	50	–692.0	–696.8	89.13	45.22	–0.08	0.62
	100	–694.6	–679.2	73.26	53.72	0.10	0.55
	200	–691.6	–661.8	72.26	39.18	0.01	0.67
	300	–689.8	–690.4	98.85	45.37	–0.20	0.62
HDI	10	–759.9	–682.0	112.2	89.60	–0.36	0.26
	50	–687.3	–667.1	89.41	68.27	–0.09	0.44
	100	–684.4	–719.8	100.7	61.18	–0.22	0.50
	200	–685.5	–671.8	88.97	41.50	–0.08	0.66
	300	–683.9	–675.6	92.40	48.30	–0.11	0.60

In the presence of HDM, HDE and HDI the profile of the impedance behaviour was altered and the inductive loop found in the absence of inhibitors disappears. It is likely because a complex mass transport mechanism intervened in the system formed by the corrosive medium/inhibitor/metal both in the liquid and corrosion inhibitor layer formed on the metal surface. This is indicative of diffusion-controlled reaction [9, 15, 17]. From the diameter of each semicircle of the Nyquist plots (Figure 4), the charge transfer resistance (R_{ct}) was determined; the values obtained are presented in Table 4.

From Table 5, similar trend is observed for all the inhibitors, at 10 ppm negative inhibition is observed, but on increasing the concentration, inhibition increases until the so called peak value phenomenon sets in. At 60°C peak performance is observed at 50 ppm but when temperature was increased to 80°C peak performance is observed at 200 ppm. Further

increase in concentration of inhibitor did not yield a commensurate increase in inhibition efficiency. This observation can be explained using the generally accepted mechanism [18].

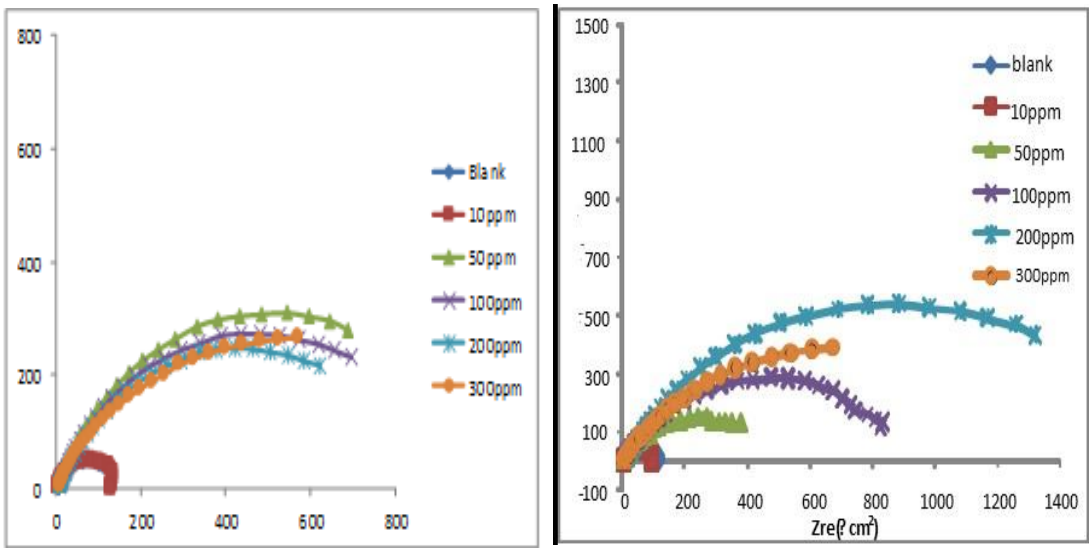

(a) (b)

Figure 4. Nyquist plots obtained at (a) 60°C and (b) 80°C for L360 mild steel in CO_2 saturated 3.5% NaCl solutions in the absence and presence of HDM.

The first step in the adsorption of an organic inhibitor on a metal surface usually involves replacement reaction of one or more water molecule adsorbed at the surface of the metal.

$$inh_{(sol)} + xH_2O_{(ads)} \leftrightarrow inh_{(ads)} + xH_2O \quad (3)$$

The inhibitor may or may not combine with freshly generated Fe^{2+} ions on the mild steel surface, forming metal–inhibitor complexes.

$$Fe \rightarrow Fe^{2+} + 2e^{-} \quad (4)$$

$$Fe^{2+} + inh_{(ads)} \rightarrow [Fe{-}inh]^{2+}_{(ads)} \quad (5)$$

The complex formed could in effect inhibit or catalyze further metal dissolution depending on its solubility.

Hence, integrity depends on environmental capacity to dilute it. Therefore, it is possible to suggest that at low concentration of 10 ppm the quantity of inhibitor in the solution was insufficient to form a compact complex with the metal ions, so that the resulting adsorbed intermediate was readily soluble in the test media. As the concentration is increased, more inhibitor molecules become available for compact complex formation, which subsequently diminishes the solubility of the surface layer, leading to improved inhibiting effect [16]. This improved inhibition could continue until a maximum is reached after which a decrease is observed in the inhibition, this is the so called peak value phenomenon.

Table 5. Inhibition efficiency using different methods.

Inhibitor	Conc. (ppm)	Weight loss method	Inhibition efficiency (%)					
			PDP method		EIS method		LPR method	
			60°C	80°C	60°C	80°C	60°C	80°C
HDM	10	71.8	–29.57	–32.38	–37.30	–10.8	–62.36	–10.27
	50		62.88	32.70	89.90	75.90	90.46	75.96
	100		32.97	68.10	82.30	79.60	82.65	80.93
	200		60.20	75.20	87.90	83.10	87.04	93.26
	300		65.89	61.30	89.50	80.60	89.98	90.79
HDE	10	60.2	–01.43	–41.90	–10.10	–21.70	–24.64	–22.40
	50		–08.72	62.70	19.60	72.20	15.66	2.13
	100		10.65	55.70	–5.80	30.20	–1.75	70.79
	200		11.61	67.70	6.90	88.00	4.75	87.45
	300		–20.57	62.60	11.80	85.60	5.99	85.02
HDI	10	65.5	–36.87	–26.20	–61.80	–21.70	–52.94	–10.53
	50		–09.07	43.80	13.10	72.20	2.52	–15.17
	100		–22.84	49.60	0.70	30.20	–8.64	12.14
	200		–08.53	65.80	2.90	88.00	–4.14	21.75
	300		–11.28	60.20	–3.30	85.60	–14.71	4.84

The effectiveness of these inhibitors has been correlated to their chemical structures the pi (π) electron of the alkyl amine substituents of the imidazoline ring in HDM are thought to play an important role in the adsorption of compounds on the metal surface, in addition to the lone pair of electrons on the nitrogen of the imidazoline compounds. Furthermore, the long straight chain/tail of the imidazoline derivatives gave steric hindrances to make the adsorption processes of this compound on the metal surface became less effective. The hydroxyethyl group on HDE was expected to give higher corrosion inhibition activity than the amine in HDI and ethylamine (aminoethyl) group in HDM, substituted on the same position, because the oxygen atom of the hydroxyethyl group has a higher electronegativity than the nitrogen atom of the amine and ethylamine group. Therefore, the affinity of the –OH group towards electrons in the 3d orbitals of a transition metal is higher than the –NH and $-NH_2$ group [11], but in this work HDM gave better inhibition than HDE and HDI this could be linked to their solubility in the test medium. This may be attributed to the minimal solubility of HDE in the test media which resulted in the inhibitors being present in low concentrations compared to the volume of

the test solutions. The concentrations were so low that they were insufficient to form a compact complex with the metal ions so that the resulting adsorbed intermediate was readily soluble in the test media thereby not providing enough scales to block the active sites to inhibit the dissolution process [16].

The dependence of the corrosion rate on temperature has been estimated using the condensed Arrhenius equation. This is to further confirm the mechanism of adsorption of the inhibitors on the mild steel surface. The Arrhenius equation is shown in Equation 6.

$$\log\left(i_{\text{corr}(2)} / i_{\text{corr}(1)}\right) = E_{\text{a}} / 2.303R\left(1/T_1 - 1/T_2\right) \tag{6}$$

where $i_{\text{corr}(1)}$ and $i_{\text{corr}(2)}$ are the corrosion currents at temperature 60°C and 80°C, respectively, E_{a} is the activation energy of the metal dissolution reaction and R is the gas constant. The E_{a} values were calculated using the i_{corr} values extrapolated from the polarization parameters obtained from the curves at 60°C (Figure 3a) and at 80°C (Figure 3b) and the calculated E_{a} values obtained for Blank is 19.19 kJ mol^{-1}, the presence of inhibitors HDM, HDE and HDI increased the activation energy thus; 48.16 kJ mol^{-1}, 33.16 kJ mol^{-1} and 23.1 kJ mol^{-1} increase in activation energy after the addition of inhibitor is synonymous with physical adsorption mechanism [18–20]. To further confirm the mechanism and the spontaneity of the adsorption process an estimate of the heat of adsorption (Q_{ads}) was obtained from the trend of surface coverage with temperature as shown in Equation 7:

$$Q_{\text{ads}} = 2.303[\log(\theta_2/1-\theta_2) - \log(\theta_1/1-\theta_1)] \times (T_1 - T_2 / T_2 - T_1) \tag{7}$$

Where Q_{ads} is the heat of adsorption, R is the gas constant, and θ_1 and θ_2 are the degrees of surface coverage of the inhibitors at the temperatures 333 and 353 K, respectively, determined using Equation 8.

$$\theta = \frac{i^0_{\text{corr}} - i_{\text{corr}}}{i^0_{\text{corr}}} \tag{8}$$

where i^0_{corr} and i_{corr} are the uninhibited and the inhibited corrosion current densities, respectively. The calculated values of Q_{ads} obtained for HDM, HDE and HDI are –58.53 kJ mol^{-1}, –103.27 kJ mol^{-1} and –133.67 kJ mol^{-1} respectively; the negative values indicate that the adsorption of the inhibitors on the mild steel surface is exothermic and consistent with the proposed physical adsorption phenomenon for the corrosion of L360 mild steel in CO_2 saturated 3.5% NaCl solution [19, 20].

The inhibition process is attributed to the formation of adsorbed films of the inhibitors via the inhibitors polycentric adsorption sites on the metal surface which protects the metal against corrosion [19–23].

3.2 Surface analysis

To further confirm the corrosion inhibition of the synthesized imidazoline derivatives, scanning electron microscope (SEM) in the range 0–200 nm was used on the surfaces of metal coupons before immersion (as polished) and 1 hour after immersion in the test solutions with and without inhibitor (blank). The obtained results are as shown in Figure 5 for HDM, HDE and HDI. The rapid corrosion attack observed for coupon immersed in the solution without inhibitor (blank) was greatly ameliorated in varying degrees in the presence of 100 ppm of the organic compounds.

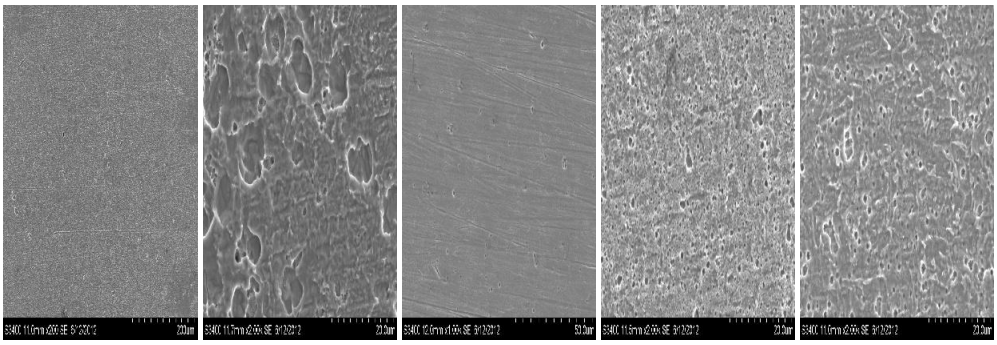

(a) (b) (c) (d) (e)

Figure 5. SEM images of (a) unexposed, (b) exposed in blank solution and (c) exposed in test solutions containing 100 ppm HDM (d) 100 ppm HDE (c) 100 ppm HDI at 80°C.

4. Conclusion

The results indicate that the synthesized compounds exhibited good corrosion inhibition properties against the corrosion of mild steel in 3.5% NaCl solutions saturated with CO_2 at 60°C and 80°C. The inhibition efficiencies of the compounds increased with increase in the inhibitors concentration to a maximum concentration value but decrease with increase in temperature. The efficiency of the compounds is in the order: HDM > HED > HDI. The corrosion inhibition efficiency of the imidazoline compounds is a function of polycentric adsorption sites on their structures.

Acknowledgement

The authors acknowledge The World Academy of Science (TWAS) for the award of 2010 TWAS fellowship for Research and Advanced Training.

Competing interests

Authors have declared that no competing interests exist.

References

1. S.C. Yoon, H. Shokrollah, N.V. Thanh, N. Srdjan, Z.B.A. Ahmad, M.N. Azmi and F. Muhammad, *NACE International Corrosion Conference and Expo*, Houston, Texas, USA, 2017, **9153**.
2. E.M. Mysara and A.A.K.A. Nurfarahin, *J. Appl. Environ. Biol. Sci*., 2017, **7**, 28.
3. A. Bouyanzer, B. Hammouti, I. Majidi and B. Haloui, *Port. Electrochim. Acta*, 2010, **28**, 165.
4. M. Elachouri, M.S. Hajji, S. Kertit, E.M. Salem and R. Coudert, *Corros. Sci*., 1995, **37**, 81.
5. B. Mernari, H. El attari, M. Traisnel, F. Bentiss and M. Lagrenee, *Corrosion*, 1998, **4**, 391.
6. L. Wang, *Corros. Sci*., 2001, **43**, 2281.
7. M.E. Azhar, M. Mernari, M. Traisnel, F. Bentiss and M. Lagrenee, *Corros. Sci*., 2001, **43**, 2229.
8. Y.J. Tan, S. Bailey and B. Kinsella, *Corros. Sci*., 1996, **38**, 1545.
9. P.C. Okafor and Y. Zheng, *Corros. Sci*., 2009, **51**, 850. doi: 10.1016/j.corsci.2009.01.027
10. J. Cruz, L.M. Martinez-Aguilera, R. Salcedo and M. Castro, *Int. J. Quantum Chem*., 2001, **85**, 546. doi: 10.1002/qua.10018
11. W. Deana, A. Sadijah, M. Yana, B. Syah and A. Bambang, *Inst. Teknol. Bandung*., 2008, **40**, 33.
12. A.Y. Usyatinsky and Y.L. Khmelnitsky, *Tetrahedron lett*., 2000, **41**, 5031.
13. I. Abdelrhman Aiad, A.A. Hafiz, M.Y. El-Awady and A.O. Habib, *J. Surfactants Deterg*., 2010, **13**, 247.
14. S. Bilgic and M. Sahin, *Mater. Chem. Phys*., 2001, **70**, 275.
15. P.C. Okafor, C.B. Liu, Y.J. Zhu and Y.G. Zheng, *Ind. Eng. Chem. Res*., 2011, **50**, 7273. doi: 10.1021/ie1024112
16. E.E. Oguzie, Y. Li and F.H. Wang, *Electrochim. Acta*, 2007, **53**, 909. doi: 10.1016/j.electacta.2007.07.076
17. E.E. Oguzie, S.G. Wang, Y. Li and F.H. Wang, *J. Phys. Chem*., 2009, **113**, 8420. doi: 10.1021/jp9015257
18. E.E. Oguzie, Y. Li and F.H. Wang, *J. Colloid Interface Sci*., 2007, **310**, 90. doi: 10.1016/j.jcis.2007.01.038
19. X. Liu, Y.G. Zheng and P.C. Okafor, *Mater. Corros*., 2009, **60**, 507. doi: 10.1002/maco.200805133
20. X. Liu, P.C. Okafor and Y.G. Zheng, *Corros. Sci*., 2009, **51**, 744. doi: 10.1016/j.corsci.2008.12.024
21. P.C. Okafor, C.B. Liu, X. Liu and Y.G. Zheng, *J. Appl. Electrochem*., 2009, **39**, 2535. doi: 10.1007/s10800-009-9948-5

22. Y.X. Qiao, Y.G. Zheng, P.C. Okafor and W. Ke, *Electrochim. Acta*, 2009, **54**, 2298. doi: 10.1016/j.electacta.2008.10.038
23. A. Frignani, M. Fonsati, C. Monticelli and G. Brunoro, *Corros. Sci*., 1999, **41**, 1217.

♦ ♦ ♦